HHS Public Access

Author manuscript

Sci Transl Med. Author manuscript; available in PMC 2022 December 03.

Published in final edited form as:

Sci Transl Med. 2020 April 22; 12(540): . doi:10.1126/scitranslmed.aaw3172.

Blocking the death checkpoint protein TRAIL improves cardiac function after myocardial infarction in monkeys, pigs, and rats

Yaohui Wang[1,*], **Hailong Zhang**[1,*], **Zhizeng Wang**[1,*], **Yinxiang Wei**[1,*], **Mingli Wang**[1], **Meichen Liu**[1], **Xuance Wang**[1,2], **Yinan Jiang**[1], **Gongning Shi**[2], **Dongmei Zhao**[2], **Zhengyan Yang**[1], **Zhiguang Ren**[1], **Jing Li**[1], **Zhenkai Zhang**[1], **Zhenfeng Wang**[1], **Bei Zhang**[1], **Beibei Zong**[1], **Xueke Lou**[1], **Chengguo Liu**[1], **Zihui Wang**[1], **Hao Zhang**[1], **Ningya Tao**[1], **Xuefang Li**[1], **Xingkun Zhang**[1], **Yafei Guo**[1], **Yang Ye**[1], **Yu Qi**[1], **Hui Li**[1], **Man Wang**[1], **Rongxin Guo**[2], **Guanchang Cheng**[2], **Shulian Li**[1], **Jun Zhang**[1], **Guangchao Liu**[1], **Lihui Chai**[1], **Qiang Lou**[1], **Xia Li**[1], **Xiukun Cui**[1], **Erhe Gao**[3], **Zheng Dong**[4], **Yanzhong Hu**[1], **Youhai H. Chen**[5,†], **Yuanfang Ma**[1,†]

[1]Joint National Laboratory for Antibody Drug Engineering, Key Laboratory of Cell and Molecular Immunology, School of Medical Sciences, Henan University, Kaifeng 475004, P.R. China.

[2]Henan University affiliated Huaihe Hospital, Kaifeng, 475004, P.R. China.

[3]Center for Translational Medicine, Temple University School, of Medicine, Philadelphia, PA 19140, USA.

[4]Department of Cellular Biology and, Anatomy, Medical College of Georgia at Augusta University and Charlie Norwood, VA Medical Center, Augusta, GA 30912, USA.

[5]Department of Pathology and Laboratory, Medicine, Perelman School of Medicine, University of Pennsylvania, Philadelphia, PA 19104, USA.

Abstract

Myocardial infarction (MI) is a leading cause of death worldwide for which there is no cure. Although cardiac cell death is a well-recognized pathological mechanism of MI, therapeutic blockade of cell death to treat MI is not straightforward. Death receptor 5 (DR5) and its ligand TRAIL [tumor necrosis factor (TNF)–related apoptosis- inducing ligand] are up-regulated in

[†]Corresponding author. mayf@henu.edu.cn (Y.M.); yhc@pennmedicine.upenn.edu (Y.H.C.).
[*]These authors contributed equally to this work.

Author contributions: Y.M. and Y.H.C. conceived the study and edited the manuscript. Y. Wang, Hailong Zhang, Zhizeng Wang, and Y. Wei designed the sDR5-Fc protein, developed methods for protein expression and characterization and NRVMs or ARVMs isolation, and established the monkey ischemic and I/R models. M.L., Mingli Wang, Zihui Wang, Hao Zhang, E.G., and Z.Z. carried out rat LAD ligations and staining. G.S., D.Z., G.C., X.W., Y.G., Man Wang, and R.G. carried out the surgeries on pigs and monkeys. Zhenfeng Wang, X.Z., B. Zong, and J.L. performed immunohistological, Masson trichrome, and TUNEL assays. C.L., and L.C. performed cell chemotaxis and Western blot studies. Y.W. and Xia Li performed flow cytometry. Z.R. and Z.Y. carried out cell deletion of macrophages and neutrophils. G.L., H.L., Q.L., and Y.Y. carried out echocardiography analysis. Y.J., N.T., X.C., and Xuefang Li performed qRT-PCR and ELISA. X. Lou, J.Z., S.L., and B. Zhang carried out primary cell isolation. Y.Q. performed protein isolation. Y. Wang analyzed the data and wrote the manuscript. Y.M., Y.H., and Z.D. supervised the project and/ or contributed to the manuscript preparation.

Competing interests: Y.M., Y. Wang, Mingli Wang, J.Z., G.L., S.L., and Y.H. hold a patent titled “Application of human sDR5 and sDR5-Fc as AMI therapeutic candidate” (ZL 2012104426856, China). Y.M., Y. Wang, Hailong Zhang, Mingli Wang, J.Z., G.L., S.L., and Y.H. hold a patent titled “sDR5-Fc fusion protein mutant and use thereof” (ZL201510510981.9, China). Y.M., Y. Wang, Hailong Zhang, Mingli Wang, J.Z., G.L., S.L., and Y.H. are inventors on patent application “sDR5-Fc fusion protein mutant and use thereof” (PCT/CN2016/081552, USA). Y.H.C. is a member of the advisory boards of Amshenn Inc. and Binde Inc. All other authors declare that they have no competing interests.

MI, but their roles in pathological remodeling are unknown. Here, we report that blocking TRAIL with a soluble DR5 immunoglobulin fusion protein diminished MI by preventing cardiac cell death and inflammation in rats, pigs, and monkeys. Mechanistically, TRAIL induced the death of cardiomyocytes and recruited and activated leukocytes, directly and indirectly causing cardiac injury. Transcriptome profiling revealed increased expression of inflammatory cytokines in infarcted heart tissue, which was markedly reduced by TRAIL blockade. Together, our findings indicate that TRAIL mediates MI directly by targeting cardiomyocytes and indirectly by affecting myeloid cells, supporting TRAIL blockade as a potential therapeutic strategy for treating MI.

INTRODUCTION

Ischemic heart disease (IHD), including myocardial infarction (MI), is a leading cause of death worldwide for which there is no cure (1, 2). An important goal for managing MI is to reestablish blood supply (reperfusion) to the injured tissue (3). However, reperfusion promotes the sequestration of inflammatory cells in ischemic tissues, the production of reactive oxygen and nitrogen species, and the development of postischemic capillary no-reflow, which amplify tissue injury (4). Ischemic and ischemia/reperfusion injuries (IRI) must be resolved to successfully manage IHD.

Mitigation of ischemic and IRI may require strategies that both protect cardiomyocytes and inhibit inflammatory cells. During MI, chemoattractants released by injured myocardium or resident immune cells recruit circulating leukocytes to the site of injury (5, 6). Neutrophils are usually the first recruited cells, which can be found in the infarcted area within 30 min of infarction. They are not only responsible for the clearance of dead cells and matrix debris but also the source of cytotoxic and inflammatory factors such as reactive oxygen species. Subsequent recruitment and activation of additional leukocytes leads to the development of inflammatory lesions seen in the infarcted tissues (7). Therefore, anti-inflammatory therapy may help control tissue injury during MI. Preclinical and/or clinical studies targeting inflammatory molecules have yielded promising results. These include strategies to block the receptor activator of nuclear factor κB (NF-κB) ligand, intercellular cell adhesion molecule–1 (ICAM-1), P-selectin, cluster of differentiation 11/18 (CD11/18), chemokine (C-C motif) receptor 2 (CCR2), C-C motif chemokine ligand 21 (CCL21), monocyte chemoattractant protein-1, tumor necrosis factor–α (TNF-α), interleukin-1β (IL-1β), and IL-6 (8–19). However, to what degree blocking inflammation alone diminishes IRI in human remains to be established (20).

Death receptor 5 (DR5 or TNFRSF10B) is the high-affinity receptor for TNF-related apoptosis-inducing ligand (TRAIL). It is closely related to the low-affinity TRAIL receptor DR4 (21). The expression of DR5 on myocardium is elevated in patients with dilated cardiomyopathy (22). The close correlation between DR5 expression and MI or heart failure has recently been established by several studies. For example, a prospective study demonstrated that DR5 is one of the most powerful biomarkers in predicting long-term all-cause mortality in patients with acute MI (AMI) (23). Similarly, proteomic profiling analysis revealed that DR5 is closely associated with systolic heart failure (24, 25). In addition, the concentration of TRAIL in the blood also correlates with the severity and outcome of MI in

patients (26–28). However, the roles of DR5 and TRAIL in MI or heart failure are unknown. We report here that the TRAIL pathway mediates ischemic and reperfusion injuries in three species including nonhuman primates and that blockade of TRAIL can prevent myocardial cell death after infarction.

RESULTS

DR5 is up-regulated in the heart during MI

To identify genes differentially regulated by ischemia and reperfusion (I/R) in the heart, we first examined the heart transcriptome by RNA sequencing (RNA-seq). We identified 1757 up-regulated and 753 down-regulated genes in rat hearts after 1 hour of ischemia and 3 hours of reperfusion (I1/R3h), as compared to the sham group. Similarly, we identified 2849 up-regulated and 2675 down-regulated genes after I1/R24h (fig. S1, A to D). DR5 was found to be up-regulated in the heart after both I1/R3h and I1/R24h, which was confirmed by quantitative reverse transcription polymerase chain reaction (qRT-PCR; fig. S1, E and F). I/R-induced DR5 up-regulation was also confirmed by protein expression in the hearts of Wistar rats, minipigs, and rhesus monkeys (fig. S2A).

Soluble DR5-Fc reduces infarct size and improves cardiac function in rodents and rhesus macaques

We hypothesized that the TRAIL-DR5 signaling pathway might be involved in IRI and that blocking TRAIL might help ameliorate pathological conditions. To test this hypothesis, we first designed a soluble DR5-Fc (sDR5-Fc) chimeric protein that contains the extracellular domain of human DR5 and the Fc domain of human immunoglobulin G1 (IgG1). The sDR5-Fc fusion protein was expressed in mammalian Chinese hamster ovary K1 (CHO-K1) cells (Huabo Biopharm Co. Ltd.), and more than 30 g of purified endotoxin-free proteins was prepared for this study (fig. S2, B and C). The sDR5-Fc bound to human, monkey, and murine TRAIL with high affinities as determined by Biacore (fig. S2D). It blocked TRAIL-induced apoptosis in a dose-dependent manner and specifically blocked the recognition of DR5 antibody for cell surface DR5 (fig. S2, E and F).

To begin to evaluate the efficacy of sDR5-Fc in vivo, we compared three doses of sDR5-Fc administered 30 min after left anterior descending (LAD) artery ligation to induce MI and IRI in rats. Treatment with 15 mg/kg resulted in the greatest reduction in infarct size compared to phosphate-buffered saline (PBS) control treatment (fig. S3). To determine the roles of TRAIL in simian AMI, myocardial ischemia was induced in adult rhesus macaques (*Macaca mulatta*) by ligating the LAD artery for 6 hours, delivering sDR5-Fc by intravenous injection 30 min after ligation; the vehicle PBS was used as a control. sDR5-Fc markedly reduced infarct size and plasma creatine kinase (CK) and lactate dehydrogenase (LDH) concentrations [$P < 0.001$ for infarction size (IS); Fig. 1, A to D]. In addition, in the I/R model in which ligation lasted for 1 hour followed by reperfusion for 6 hours (I1/R6h), sDR5-Fc showed strong protective effect against infarction and significantly reduced plasma CK, LDH, and cardiac troponin I (cTnI) concentrations ($P < 0.001$ for IS; Fig. 1, E to H). The protective effect of sDR5 against infarction in monkeys was also confirmed by single-photon emission tomography/computed tomography (Fig. 1I).

To determine whether TRAIL blockade improved long-term heart function in monkeys, echocardiography was performed every 14 days from days 30 to 90 after permanent ligation of the LAD artery. The result demonstrated that sDR5-Fc significantly preserved the ejection fraction (EF) and fractional shortening (FS) index at day 60 after MI, and the protective effect lasted for at least 90 days ($P = 0.0188$ for EF and $P = 0.0122$ for FS; Fig. 1, J to L). sDR5-Fc also reduced fibrosis and prevented thinning of the ventricular wall (Fig. 1, M and N).

sDR5-Fc protects against MI in minipigs

The anatomical structure and organ size of pig hearts are very close to those of humans. We therefore tested the effect of TRAIL blockade on AMI and IRI in minipigs. We found that sDR5-Fc markedly reduced infarct size in both AMI (6 hours) and I1/R6h models ($P < 0.001$ for both groups; Fig. 2, A and E). As expected, the plasma CK, LDH, and cTnI were all significantly decreased by sDR5-Fc in both AMI and I/R models (Fig. 2, B and C and F to H). We also observed a slight decrease of cTnI concentration in sDR5-Fc–treated AMI model (Fig. 2D). These results demonstrated that sDR5-Fc protected porcine heart against both ischemic and IRI.

TRAIL blockade or DR5 deletion alleviates MI and improves cardiac function in rats

To investigate the underlying mechanism of the therapeutic effect of sDR5-Fc in MI, we next turned to rodent models of AMI and I/R. We found that in the AMI (6 hours) model of Wistar rats, sDR5-Fc significantly reduced infarct size [$P = 0.0014$ for IS/area at risk (AAR) group; Fig. 3A]. Similarly, in both the I1/R3h and I1/R24h models, sDR5-Fc significantly reduced infarct size ($P < 0.001$ for I1/R3h IS/AAR group and $P = 0.0326$ for I1/R24h IS/AAR group; Fig. 3, B and C) and serum cTnI (I1/R3h group; Fig. 3D). The improvement in cardiac function by sDR5-Fc was also observed 4 weeks after LAD artery ligation by echocardiography, consistent with a decrease in fibrosis (Fig. 3, E to H). The protective effect of TRAIL blockade in rats was further confirmed by administering a blocking anti-DR5 monoclonal antibody (mAb) 5 min before reperfusion in the I1/R24h model (fig. S4).

To determine whether specifically blocking TRAIL receptor with sDR5-Fc produced optimal cardioprotection, we compared several controls: PBS (vehicle control), human IgG (protein control), and etanercept (human TNF receptor–Fc; TNF receptor family control). PBS and human IgG had no detectable effect, whereas etanercept reduced infarct size in rats when administered 5 min before reperfusion in the I1/R24h model (Fig. 3I). When used in combination, sDR5-Fc and etanercept conferred the best myocardial protection (Fig. 3I). To directly test the roles of the TRAIL-DR5 pathway in IRI, we generated DR5 knockout rats using CRISPR-Cas9–mediated gene targeting (fig. S5) and challenged them with 1 hour ischemia and 24 hours reperfusion (I1/R24h). Compared to wild-type control rats, DR5 knockout rats developed smaller infarcts ($P < 0.001$ for IS/AAR group; Fig. 3J). Thus, the TRAIL-DR5 pathway plays a crucial role in IHD.

The myocardial protective effect of sDR5-Fc is time-dependent

To determine the therapeutic window of sDR5-Fc administration for treating MI, we examined the temporal effect of sDR5-Fc on I/R in both rats and monkeys. For rats, the

anterior coronary artery was ligated for 3 or 4 hours followed by reperfusion for 24 hours, and sDR5-Fc was administered 1 hour after artery ligation. The results showed that sDR5-Fc could significantly reduce cardiac damage in hearts subjected to 3 hours, but not 4 hours, of ischemia ($P < 0.001$ for I3/R24h and $P = 0.8922$ for I4/R24h; Fig. 4A). sDR5-Fc administration could be delayed 1.5 hours, but not 3 hours, after artery ligation to achieve a significant protective effect ($P = 0.013$ for I1.5/R24h and $P = 0.2926$ for I3/R24h; Fig. 4B). For rhesus monkeys, the anterior coronary artery was ligated for 2 or 3 hours followed by reperfusion for 6 hours; sDR5-Fc was administered 1 hour after ligation for duration of 3-hour ligation or 2 hours after ligation. The results showed that sDR5-Fc could significantly reduce cardiac damage under both of these conditions ($P < 0.001$ for I3/R6h and $P = 0.0037$ for I2/R6h; Fig. 4, C and D). Thus, our results indicate that sDR5-Fc could significantly protect heart tissue from ischemic injury if administered within 2 hours of the ischemia.

sDR5-Fc blocks TRAIL-induced cardiomyocyte death directly

Death of cardiomyocytes is an essential mechanism of pathological remodeling after MI. Because DR5 was up-regulated in ischemic hearts, we speculated that TRAIL might directly induce the death of cardiomyocytes. Compared to the control groups, using TUNEL (terminal deoxynucleotidyl transferase–mediated deoxyuridine triphosphate nick end labeling) staining, we detected fewer apoptotic cells in the hearts of rats in the sDR5-Fc–treated groups 3 and 24 hours after artery ligation ($P = 0.0117$ for I1/R3h and $P < 0.001$ for I1/R24h; Fig. 5A). Similarly, we detected reduced caspase 3 and caspase 8 activation in sDR5-Fc–treated groups by immunohistochemistry (IHC) and immunoblotting (Fig. 5, B to E, and fig. S6, A to C). The mitochondria pathway of cell death could cross-talk with the death receptor pathway (29). Blocking TRAIL also affected expression of Bak and Bax, two key players of the mitochondria pathway, after cardiac ischemia (fig. S7A).

We next examined whether sDR5-Fc could directly block TRAIL-induced death of rat and human cardiomyocytes in culture. TRAIL-induced TUNEL signals and caspase 3/7 activation in neonatal rat ventricular myocytes (NRVMs) were markedly reduced by sDR5-Fc treatment after 2 hours of hypoxia and 3 hours of reoxygenation (H2/R3h; Fig. 5, F and G). By contrast, TRAIL showed no detectable effect on NRVMs under normoxic condition (fig. S7B). Similarly, sDR5-Fc eliminated hypoxia/reoxygenation (H/R)– and TRAIL-induced death of NRVMs and adult rat ventricular myocytes (ARVMs) as determined by time-lapse microscopy (Fig. 5, H and I, and fig. S8). Apoptosis of human primary ventricular cardiomyocytes was also significantly inhibited by sDR5-Fc as determined by TUNEL, caspase 3/7 assays, and time-lapse microscopy (Fig. 5, J and K, and fig. S8). These results indicate that sDR5-Fc can reverse TRAIL-mediated cardiomyocyte apoptosis because of H/R injury.

The myocardial protective effect of sDR5-Fc during I/R is myeloid cell dependent

Myeloid cell–mediated inflammation plays a crucial role in I/R. Using RNA-seq, we detected a large number of genes up-regulated in the hearts of rats exposed to I1/R3h or I1/R24h as compared to sham controls (tables S1 and S2). Among the induced genes, inflammatory cytokines were one of the most significantly up-regulated clusters (Fig. 6, A and B). By qRT-PCR, we confirmed the increase of many inflammatory mRNAs,

which include *IL-1*β, *IL-6*, *TNF*-α, *ICAM-1*, and *IL-18* (Fig. 6, C to G). Myeloid cell infiltration is a key pathological feature of IRI. sDR5-Fc significantly reduced the infiltration of both neutrophils and monocytes as compared to the control group [$P = 0.0071$ for myeloperoxidase-positive (MPO^+) I1/R3h group, $P < 0.001$ for MPO^+ I1/R24h group, $P = 0.0042$ for $CD68^+$ I1/R3h group, and $P < 0.001$ for $CD68^+$ I1/R24h group; Fig. 6, H and I, and fig. S9, A and B].

To determine the potential roles of myeloid cells in sDR5-mediated therapeutic effects on MI, we depleted them in rats using antineutrophil antibodies and clodronate liposomes (for monocytes/macrophages) before I/R. Depleting either neutrophils or monocytes/macrophages reduced the infarct size but completely abolished the protective effect of sDR5-Fc ($P < 0.001$ for normal rabbit serum group, $P = 0.9218$ for anti-polymorphonuclear leukocytes group, $P < 0.001$ for PBS liposomes group, and $P = 0.6684$ for CL group; Fig. 6, J and K, and fig. S10, A to E). Next, we examined the effect of H/R and/or TRAIL stimulation on monocytes/macrophages. Hypoxia/reoxygenation injury induced the expression of *IL-1*β, *TNF*-α, *IL-6*, and *ICAM-1* mRNA in the rat macrophage cell line NR8383, which was blocked by sDR5-Fc (Fig. 6, L to O). Similar effects were seen when isolated cardiac infiltrating myeloid cells were treated with sDR5-Fc (Fig. 6, P to S). These findings indicated that the protective effects of sDR5-Fc against IRI require the presence of myeloid cells.

sDR5-Fc blocks myeloid cell migration

Previously, we reported that TRAIL induces cytokine expression and release in macrophages during H/R (30). During myocardial I/R, both immune cells and nonimmune cells are the potential source of TRAIL (fig. S11). Using a Transwell assay, we found that TRAIL promoted NR8383 macrophage migration in a dose-dependent manner (Fig. 7, A and B). As expected, sDR5-Fc dose-dependently blocked the migration of NR8383 macrophages and primary rat bone marrow–derived macrophages (BMDMs; Fig. 7, C to F). Left ventricle heart tissue from rats subjected to I1/R24 showed increased *CCL-2* expression (Fig. 7G), and NR8383 macrophages subjected to H/R and BMDMs treated with TRAIL similarly up-regulated CCL-2 (Fig. 7, H and I); treatment with sDR5-Fc reduced CCL-2 expression in each model. In addition, the increased expression of the CCL-2 receptor *CCR2* in injured rat heart tissue and TRAIL-challenged NR8383 macrophages could be lowered by treatment with sDR5-Fc (Fig. 7, J and K). These findings suggested that TRAIL promotes myeloid cell migration during I/R either directly or indirectly by up-regulating chemokines and/or their receptors.

DISCUSSION

TRAIL, a member of the TNF superfamily, was initially thought to preferentially induce apoptosis of cancer cells but not noncancerous cells. However, the results of clinical trials for TRAIL in cancer therapy were not as impressive as initially hoped (31). In recent years, a growing number of studies indicate that TRAIL may play important roles in nonneoplastic diseases including inflammatory and cardiovascular diseases (32–37). In addition to inducing cell death, TRAIL can also activate proinflammatory and

survival pathways through NF-κB and phosphatidylinositol 3-kinase and promote cytokine expression and secretion (38). However, whether TRAIL plays a role in the death of cardiomyocytes during health or disease was previously unknown.

Although TRAIL can induce apoptosis in benign cells, cardiomyocytes may differ considerably from tumor cells in their sensitivity to TRAIL-induced death under hypoxic conditions. Whether hypoxia increases or decreases TRAIL-induced death of cancer cells is not completely understood. Although several reports indicate that TRAIL-induced tumor cell death is enhanced by hypoxia (39, 40), others observed the opposite effect (41–43). A close examination of these reports indicates that different cancer cells may differ considerably in their sensitivity to TRAIL under hypoxia, presumably depending on expression of B-cell CLL/lymphoma 2 (Bcl-2), X-linked inhibitor of apoptosis (XIAP), hypoxia inducible factor-1α (Hif-1α), caspase 8, and DR5. Thus, hypoxia may regulate TRAIL-induced cell death in a cancer cell–specific manner (44).

Here, we investigated the effect of TRAIL blockade on cardiac infarction using multiple animal models and cell culture. We found protective effect of sDR5-Fc that may relate to both apoptosis inhibition and reduction of inflammation. There are several types of immune cells that sequentially or synergistically contribute to cell damage after MI, which include neutrophils, monocytes/macrophages, T cells, and natural killer (NK) cells. RNA interference targeting of multiple cell adhesion molecules has been shown to reduce post-MI neutrophil and monocyte recruitment into atherosclerotic lesions and decrease matrix-degrading plaque protease activity (45). Dectin-1, an NK receptor, was found to play an important role in myocardial IRI by regulating macrophage and neutrophil infiltration (46). Here, we found that monocytes/macrophages and granulocytes are required for the protective effects of sDR5-Fc. During I/R, these cells could cause myocardial injury directly through their TRAIL expression or indirectly through secretion of inflammatory molecules: Both of these processes can be blocked by sDR5-Fc. TRAIL can promote monocyte chemotaxis by binding DR4 (47). Anti- inflammatory therapies targeting cytokines such as TNF-α, IL-6, and IL-1β may help ameliorate IRI (19, 48). However, although effective in animals, TNF blockers showed no clinical benefit in human chronic heart failure and AMI trials (including the well- publicized RENAISSANCE, RECOVER, and RENEWAL trials) (49). Cross-species differences in genes and living conditions are major barriers for translating animal research to humans. For this reason, we tested the effect of the sDR5-Fc in three species including nonhuman primates. Because our sDR5-Fc is of human origin, its affinity to human and monkey TRAIL is at least 10 times higher than that to rat TRAIL, which may explain why it was more effective in protecting monkey hearts than rat hearts. It is worth mentioning that no arrhythmia or sudden death was observed after permanent ligation of the LAD artery up to 60 days in our monkey study. Because sDR5-Fc not only blocks TRAIL-induced cell death but also decreases the expression of IL-1β and IL-6, it will likely be more effective than strategies targeting a single inflammatory cytokine.

The cellular source of TRAIL involved in myocardial I/R is not entirely clear. Immune cells, which include monocytes/macrophages, neutrophils, T cells, and NK cells, are generally the main source of TRAIL. Cardiac-resident cells including fibroblasts and endothelial cells might also be a potential source of TRAIL. In addition to cell membrane–bound

TRAIL, soluble TRAIL, which is likely generated through matrix metalloproteinase 2 cleavage of membrane-bound TRAIL, can be detected in blood or tissue fluid (50). Blood concentrations of soluble TRAIL negatively correlated with MI outcome (28). It is plausible that I/R-induced up-regulation of DR5 effectively reduces soluble TRAIL in circulation.

In summary, using an sDR5-Fc fusion protein that specifically blocks the TRAIL pathway, we demonstrated its strong cardioprotective effect in rats, pigs, and nonhuman primates. Blocking TRAIL simultaneously reduced cardiomyocyte death and inflammation in animal models and represents a potential strategy to treat MI. However, it should be emphasized that translating animal research into the clinic remains a challenging task. Previous animal studies targeting cell death or inflammatory regulators such as CD18 showed impressive effects in models of MI but failed to protect human patients with MI in clinical trials (13, 51). The potential therapeutic benefit of sDR5-Fc in humans with MI will require future clinical trials.

MATERIALS AND METHODS

Study design

The purpose of this study was to assess the cardiac protective effect of an sDR5-Fc fusion protein and to elucidate its underlying mechanisms of action in three species. To better guide potential future clinical trials in humans, rat, pig, and monkey models of MI, including both ischemia and I/R, were treated with sDR5-Fc. We evaluated several regimens of administration (dosing and timing of treatment). Primary cardiac cells, including human cardiomyocytes, were used to dissect the mechanisms of TRAIL-mediated effects during H/R. The effect of TRAIL on myeloid cells was also studied by Transwell assays, qRT-PCR, and enzyme-linked immunosorbent assay (ELISA).

For in vivo work, after anesthesia, rats, pigs, and monkeys were randomized to receive PBS or sDR5-Fc injection. For rats, LAD ligation, sDR5-Fc treatment, and tetraphenyl tetrazolium chloride (TTC)–Evans blue staining were performed by laboratory technologists, and the infarct sizes were assessed by separate researchers blinded to the treatment conditions. For pigs and monkeys, cardiac procedures and sDR5-Fc treatment were performed by senior cardiac surgeons; cardiac functional assessments (echocardiography) were performed and interpreted by echocardiologists blinded to the treatment. All histological sections were immunostained and analyzed by separate researchers blinded for the treatment. Imaging studies for TTC and IHC, immunoblots, and quantitative PCR were repeated at least three times. For all other in vivo and in vitro studies, the numbers of repeats are indicated in the figure legends. The sequence of primers used in this study was presented in table S3. The study results were reported in accordance with the Animal Research: Reporting In Vivo Experiments (ARRIVE) guidelines. All animal experiments were conducted in adherence with the Guidelines of Welfare and Ethics for the Use of Laboratory Animals, China. All animal procedures were preapproved by the Animal Care and Use Committee of the Henan University, China.

Animals

Male (9 to 11 kg) and female (5 to 7 kg) rhesus macaques (10 to 12 years of age) were purchased from Xinyu Wild Animal Breeding Co. Male and female Bama pigs (~20 kg, 2 to 3 months of age) were purchased from Taihe Biotechnology Co. Monkeys and pigs were housed in individual cages and acclimatized to the laboratory condition for a period of 2 to 4 weeks. Male Wistar rats (220 to 250 g, 7 to 8 weeks) were purchased from Beijing Vital River Laboratory Animal Technology Co. DR5 knockout Sprague-Dawley rats were generated by the Wuhan University Center for Laboratory Animals using CRISPR-Cas9–mediated gene targeting (52). The $Dr5^{-/-}$ homozygote line was obtained at F2 generation, which expressed no DR5 mRNA or protein as determined by RT-PCR and immunoblotting, respectively. Rats were acclimated for 7 days before any experimental procedures. All animals were housed with free access to water and food with a 12-hour light/12-hour dark cycle at 25°C.

Production and validation of sDR5-Fc

sDR5-Fc was designed to contain the extracellular fragment of human DR5 (amino acids 1 to 182) and the human IgG1 Fc fragment. It was expressed in CHO-K1 cells by stable transfection and purified from culture supernatant using Protein A affinity column (53). The quality of the purified protein was assessed by SDS–polyacrylamide gel electrophoresis and high-performance liquid chromatography (Shimadzu). Endotoxins were measured using a Limulus amebocyte lysate assay (Xiamen Bioendo Technology Co. Ltd.). Flow cytometry was performed to examine the blocking effect of sDR5-Fc on TRAIL-induced Jurkat cell apoptosis after staining cells with annexin V and propidium iodide (KeyGen Biotech). The binding activity of sDR5-Fc with human and murine TRAIL was measured by Biacore (X100, GE Life Sciences), with TRAIL precoated on the bottom of the chip. Association rates (K_a) and dissociation rates (K_d) were acquired by a simple 1:1 binding model. The equilibrium dissociation constants (K_D) was calculated as the ratio of K_d and K_a ($K_D = K_d/K_a$).

The rat MI model

For the I/R model, rats were anesthetized through intraperitoneal administration of sodium pentobarbital (60 mg/kg). Under artificial ventilation with a rodent ventilator, a left thoracotomy was performed. The proximal portion of the left coronary artery was surgically occluded for 60 min through ligation with a suture (size, 5–0), followed by coronary reperfusion through release of the tie. Coronary occlusion was confirmed through elevation of the ST segment on the electrocardiogram (ECG). sDR5-Fc was administrated by single dose through tail vein injection. After coronary reperfusion, the tie was left loose on the surface of the heart; the chest was closed, followed by intratracheal tube and ECG electrodes removal. At the respective time after coronary reperfusion, 0.5 ml of blood was obtained from the jugular vein for analysis. Then, an intratracheal tube was inserted, and the chest was reopened under artificial ventilation. The coronary artery was again briefly occluded through ligation of the tie that remained at the site of the previous occlusion. Immediately after the ligation, 2% Evans blue solution was infused into aorta to delineate the ischemic AAR of the left ventricle. After administration of an excessive dose of sodium pentobarbital

into the peritoneal cavity, the heart was excised and cross-sectioned from the apex to the occlusion site into five specimens of about 2 mm in thickness, followed by incubation in 1% (0.01 g/ml) TTC in PBS at 37°C for 20 min. The heart slices were photographed with a digital camera to distinguish the red-stained viable tissues and the white- unstained necrotic tissues. Areas of infarct size were digitally measured using ImageJ software.

For AMI model, the LAD coronary artery was ligated for 6 hours before sacrifice. For the heart remodeling model, LAD coronary artery was ligated for 4 weeks, heart function was monitored by echocardiography at 2 and 4 weeks, and the fibrosis was detected by Masson's trichrome staining.

The pig and monkey MI models

For AMI model, Bama pigs were fasted for 12 hours and water-deprived for 4 hours. After anesthesia induction by ketamine [5 mg/kg, intramuscular (im)] and midazolam (0.5 mg/kg, im), the pigs were fixed on the operating table, and the ear intravenous drip was performed. The pigs were then anesthetized intravenously with propofol (3 mg/kg), sufentanil (1 μg/kg), and vecuronium (0.1 mg/kg), and respiration was maintained through endotracheal intubation by a respirator, which steadily exported isoflurane (1.0 minimal alveolar concentration). A median sternotomy was performed to expose the heart. Subsequently, the pericardium was scratched, and the LAD coronary artery was ligated with a 5–0 nonabsorbable surgical suture. The location was 1 to 2 mm above the second diagonal artery. The pericardium and sternum were separately seamed with 3–0 and 0–0 surgical sutures. The skin incision was also closed with 3–0 sutures. Thirty minutes after the ligation, the pigs were randomly divided into two groups, which were administrated PBS or sDR5-Fc (8 mg/kg) intravenously. Lidocaine was intravenously administrated to prevent ventricular fibrillation.

For the pig I/R model, anesthesia and surgery were performed as described for the AMI model. One hour later, the LAD ligation was loosened to allow reperfusion. PBS or sDR5-Fc was administrated via ear vein 5 min before reperfusion. For monkey AMI and I/R models, the anesthesia and surgical procedures were performed as described above for pigs, except that the thoracotomy incision was performed between the fourth and fifth ribs, and sDR5-Fc (6 mg/kg) was injected into the dorsal veins of the hand. Plasma CK and LDH concentrations were analyzed using the Catalyst DX analyzer (IDEXX) following the manufacturer's instructions.

Statistical analysis

Data are presented as means ± SEM. Statistical significance was determined by the unpaired Student *t* test for two groups and one-way analysis of variance (ANOVA) for multiple groups using SPSS 16.0 software. Raw data are reported in data file S1.

Supplementary Material

Refer to Web version on PubMed Central for supplementary material.

Acknowledgments:

We thank D.Y. Wang for excellent technical assistance and W.Z. Tian for generating the CHO-K1 stable line and for sDR5-Fc protein purification.

Funding:

This work was supported by the National Natural Science Foundation of China (nos. 81670271, U1404801, and U1404801) and Foundation of Henan Educational Committee (no. 14A416008).

Data and materials availability:

All data associated with this study are present in the paper or the Supplementary Materials.

REFERENCES AND NOTES

1. Hayman KG, Sharma D, Wardlow RD, Singh S, Burden of cardiovascular morbidity and mortality following humanitarian emergencies: A systematic literature review. Prehosp. Disaster Med 30, 80–88 (2015). [PubMed: 25499440]
2. Lefer DJ, Marban E, Is cardioprotection dead? Circulation 136, 98–109 (2017). [PubMed: 28674094]
3. Thiele H, Desch S, de Waha S, Acute myocardial infarction in patients with ST-segment elevation myocardial infarction: ESC guidelines 2017. Herz 42, 728–738 (2017). [PubMed: 29119223]
4. Kalogeris T, Baines CP, Krenz M, Korthuis RJ, Ischemia/reperfusion. Comp. Physiol 7, 113–170 (2016).
5. Frangogiannis NG, Pathophysiology of myocardial infarction. Compr. Physiol 5, 1841–1875 (2015). [PubMed: 26426469]
6. Yan X, Anzai A, Katsumata Y, Matsuhashi T, Ito K, Endo J, Yamamoto T, Takeshima A, Shinmura K, Shen W, Fukuda K, Sano M, Temporal dynamics of cardiac immune cell accumulation following acute myocardial infarction. J. Mol. Cell. Cardiol 62, 24–35 (2013). [PubMed: 23644221]
7. Bonaventura A, Montecucco F, Dallegri F, Cellular recruitment in myocardial ischaemia/reperfusion injury. Eur. J. Clin. Invest 46, 590–601 (2016). [PubMed: 27090739]
8. Carbone F, Crowe LA, Roth A, Burger F, Lenglet S, Braunersreuther V, Brandt KJ, Quercioli A, Mach F, Vallee JP, Montecucco F, Treatment with anti-RANKL antibody reduces infarct size and attenuates dysfunction impacting on neutrophil-mediated injury. J. Mol. Cell. Cardiol 94, 82–94 (2016). [PubMed: 27056420]
9. Squadrito F, Altavilla D, Squadrito G, Saitta A, Deodato B, Arlotta M, Minutoli L, Quartarone C, Ferlito M, Caputi AP, Tacrolimus limits polymorphonuclear leucocyte accumulation and protects against myocardial ischaemia- reperfusion injury. J. Mol. Cell. Cardiol 32, 429–440 (2000). [PubMed: 10731442]
10. Stähli BE, Gebhard C, Duchatelle V, Cournoyer D, Petroni T, Tanguay J-F, Robb S, Mann J, Guertin M-C, Wright RS, L'Allier PL, Tardif J-C, Effects of the P-selectin antagonist inclacumab on myocardial damage after percutaneous coronary intervention according to timing of infusion: Insights from the SELECT-ACS trial. J. Am. Heart Assoc 5, e004255 (2016).
11. Dewald O, Zymek P, Winkelmann K, Koerting A, Ren G, Abou-Khamis T, Michael LH, Rollins BJ, Entman ML, Frangogiannis NG, CCL2/monocyte chemoattractant protein-1 regulates inflammatory responses critical to healing myocardial infarcts. Circ. Res 96, 881–889 (2005). [PubMed: 15774854]
12. Jiang Y, Bai J, Tang L, Zhang P, Pu J, Anti-CCL21 antibody attenuates infarct size and improves cardiac remodeling after myocardial infarction. Cell. Physiol. Biochem 37, 979–990 (2015). [PubMed: 26393504]
13. Faxon DP, Gibbons RJ, Chronos NAF, Gurbel PA, Sheehan F; HALT-MI Investigators, The effect of blockade of the CD11/CD18 integrin receptor on infarct size in patients with acute myocardial infarction treated with direct angioplasty: The results of the HALT-MI study. J. Am. Coll. Cardiol 40, 1199–1204 (2002). [PubMed: 12383565]

14. Hayashidani S, Tsutsui H, Shiomi T, Ikeuchi M, Matsusaka H, Suematsu N, Wen J, Egashira K, Takeshita A, Anti-monocyte chemoattractant protein-1 gene therapy attenuates left ventricular remodeling and failure after experimental myocardial infarction. Circulation 108, 2134–2140 (2003). [PubMed: 14517168]
15. Hartman MHT, Groot HE, Leach IM, Karper JC, van der Harst P, Translational overview of cytokine inhibition in acute myocardial infarction and chronic heart failure. Trends Cardiovasc. Med 28, 369–379 (2018). [PubMed: 29519701]
16. Padfield GJ, Din JN, Koushiappi E, Mills NL, Robinson SD, Le May Cruden N, Lucking AJ, Chia S, Harding SA, Newby DE, Cardiovascular effects of tumour necrosis factor α antagonism in patients with acute myocardial infarction: A first in human study. Heart 99, 1330–1335 (2013). [PubMed: 23574969]
17. Holte E, Kleveland O, Ueland T, Kunszt G, Bratlie M, Broch K, Michelsen AE, Bendz B, Amundsen BH, Aakhus S, Damas JK, Gullestad L, Aukrust P, Wiseth R, Effect of interleukin-6 inhibition on coronary microvascular and endothelial function in myocardial infarction. Heart 103, 1521–1527 (2017). [PubMed: 28432157]
18. Ridker PM, MacFadyen JG, Everett BM, Libby P, Thuren T, Glynn RJ; CANTOS Trial Group, Relationship of C-reactive protein reduction to cardiovascular event reduction following treatment with canakinumab: A secondary analysis from the CANTOS randomised controlled trial. Lancet 391, 319–328 (2018). [PubMed: 29146124]
19. Ridker PM, Everett BM, Thuren T, MacFadyen JG, Chang WH, Ballantyne C, Fonseca F, Nicolau J, Koenig W, Anker SD, Kastelein JJP, Cornel JH, Pais P, Pella D, Genest, Cifkova R, Lorenzatti A, Forster T, Kobalava Z, Vida-Simiti L, Flather M, Shimokawa H, Ogawa H, Dellborg M, Rossi PRF, Troquay RPT, Libby P, Glynn RJ; CANTOS Trial Group, Antiinflammatory therapy with canakinumab for atherosclerotic disease. N. Engl. J. Med 377, 1119–1131 (2017). [PubMed: 28845751]
20. Huet F, Akodad M, Fauconnier J, Lacampagne A, Roubille F, Anti-inflammatory drugs as promising cardiovascular treatments. Expert Rev. Cardiovasc. Ther 15, 109–125 (2017). [PubMed: 28010154]
21. Micheau O, Regulation of TNF-related apoptosis-inducing ligand signaling by glycosylation. Int. J. Mol. Sci 19, E715 (2018).
22. Dzimiri N, Afrane B, Canver CC, Preferential existence of death-inducing proteins in the human cardiomyopathic left ventricle. J. Surg. Res 142, 227–232 (2007). [PubMed: 17706969]
23. Skau E, Henriksen E, Wagner P, Hedberg P, Siegbahn A, Leppert J, GDF-15 and TRAIL-R2 are powerful predictors of long-term mortality in patients with acute myocardial infarction. Eur. J. Prev. Cardiol 24, 1576–1583 (2017). [PubMed: 28762762]
24. Hage C, Michaëlsson E, Linde C, Donal E, Daubert J-C, Gan L-M, Lund LH, Inflammatory biomarkers predict heart failure severity and prognosis in patients with heart failure with preserved ejection fraction: A holistic proteomic approach. Circ. Cardiovasc. Genet 10, e001633 (2017).
25. Stenemo M, Nowak C, Byberg L, Sundstrom J, Giedraitis V, Lind L, Ingelsson E, Fall T, Ärnlöv J, Circulating proteins as predictors of incident heart failure in the elderly. Eur. J. Heart Fail 20, 55–62 (2018). [PubMed: 28967680]
26. Nakajima H, Yanase N, Oshima K, Sasame A, Hara T, Fukazawa S, Takata R, Hata K, Mukai K, Yamashina A, Mizuguchi J, Enhanced expression of the apoptosis inducing ligand TRAIL in mononuclear cells after myocardial infarction. Jpn. Heart J 44, 833–844 (2003). [PubMed: 14711179]
27. Osmancik P, Teringova E, Tousek P, Paulu P, Widimsky P, Prognostic value of TNF-related apoptosis inducing ligand (TRAIL) in acute coronary syndrome patients. PLOS ONE 8, e53860 (2013).
28. Secchiero P, Corallini F, Ceconi C, Parrinello G, Volpato S, Ferrari R, Zauli G, Potential prognostic significance of decreased serum levels of TRAIL after acute myocardial infarction. PLOS ONE 4, e4442 (2009). [PubMed: 19221598]
29. Gottlieb RA, Cell death pathways in acute ischemia/reperfusion injury. J. Cardiovasc. Pharmacol. Ther 16, 233–238 (2011). [PubMed: 21821521]

30. Jiang Y, Chen X, Fan M, Li H, Zhu W, Chen X, Cao C, Xu R, Wang Y, Ma Y, TRAIL facilitates cytokine expression and macrophage migration during hypoxia/reoxygenation via ER stress-dependent NF-κB pathway. Mol. Immunol 82, 123–136 (2017). [PubMed: 28073079]

31. von Karstedt S, Montinaro A, Walczak H, Exploring the TRAILs less travelled: TRAIL in cancer biology and therapy. Nat. Rev. Cancer 17, 352–366 (2017). [PubMed: 28536452]

32. Bernardi S, Bossi F, Toffoli B, Fabris B, Roles and clinical applications of OPG and TRAIL as biomarkers in cardiovascular disease. Biomed. Res. Int 2016, 1752854 (2016).

33. Harper E, Forde H, Davenport C, Rochfort KD, Smith D, Cummins PM, Vascular calcification in type-2 diabetes and cardiovascular disease: Integrative roles for OPG, RANKL and TRAIL. Vascul. Pharmacol 82, 30–40 (2016). [PubMed: 26924459]

34. Cheng W, Zhao Y, Wang S, Jiang F, Tumor necrosis factor-related apoptosis-inducing ligand in vascular inflammation and atherosclerosis: A protector or culprit? Vascul. Pharmacol 63, 135–144 (2014). [PubMed: 25451562]

35. Di Bartolo BA, Cartland SP, Prado-Lourenco L, Griffith TS, Gentile C, Ravindran J, Azahri NS, Thai T, Yeung AW, Thomas SR, Kavurma MM, Tumor necrosis factor–related apoptosis-inducing ligand (TRAIL) promotes angiogenesis and ischemia-induced neovascularization via NADPH oxidase 4 (NOX4) and nitric oxide–dependent mechanisms. J. Am. Heart Assoc 4, e002527 (2015).

36. Harith HH, Di Bartolo BA, Cartland SP, Genner S, Kavurma MM, Insulin promotes vascular smooth muscle cell proliferation and apoptosis via differential regulation of tumor necrosis factor-related apoptosis-inducing ligand. J. Diabetes 8, 568–578 (2016). [PubMed: 26333348]

37. Chan J, Prado-Lourenco L, Khachigian LM, Bennett MR, Di Bartolo BA, Kavurma MM, TRAIL promotes VSMC proliferation and neointima formation in a FGF-2−, Sp1 phosphorylation−, and NFκB-dependent manner. Circ. Res 106, 1061–1071 (2010). [PubMed: 20150555]

38. Tang W, Wang W, Zhang Y, Liu S, Liu Y, Zheng D, Tumour necrosis factor-related apoptosis-inducing ligand (TRAIL)-induced chemokine release in both TRAIL-resistant and TRAIL-sensitive cells via nuclear factor B. FEBS J. 276, 581–593 (2009). [PubMed: 19120450]

39. Lee YJ, Moon MS, Kwon SJ, Rhee JG, Hypoxia and low glucose differentially augments TRAIL-induced apoptotic death. Mol. Cell. Biochem 270, 89–97 (2005). [PubMed: 15792357]

40. Hong S-E, Kim CS, An S, Kim H-A, Hwang S-G, Song J-Y, Lee JK, Hong J, Kim J-I, Noh WC, Jin H-O, Park I-C, TRAIL restores DCA/metformin-mediated cell death in hypoxia. Biochem. Biophys. Res. Commun 478, 1389–1395 (2016). [PubMed: 27569287]

41. Nagaraj NS, Vigneswaran N, Zacharias W, Hypoxia inhibits TRAIL-induced tumor cell apoptosis: Involvement of lysosomal cathepsins. Apoptosis 12, 125–139 (2007). [PubMed: 17136492]

42. Jeong J-K, Moon M-H, Seo J-S, Seol J-W, Park S-Y, Lee Y-J, Hypoxia inducing factor-1α regulates tumor necrosis factor-related apoptosis-inducing ligand sensitivity in tumor cells exposed to hypoxia. Biochem. Biophys. Res. Commun 399, 379–383 (2010). [PubMed: 20659427]

43. Kim M, Park SY, Pai HS, Kim TH, Billiar TR, Seol DW, Hypoxia inhibits tumor necrosis factor-related apoptosis-inducing ligand-induced apoptosis by blocking Bax translocation. Cancer Res. 64, 4078–4081 (2004). [PubMed: 15205314]

44. de Looff M, de Jong S, Kruyt FAE, Multiple interactions between cancer cells and the tumor microenvironment modulate TRAIL signaling: Implications for TRAIL receptor targeted therapy. Front. Immunol 10, 1530 (2019). [PubMed: 31333662]

45. Sager HB, Dutta P, Dahlman JE, Hulsmans M, Courties G, Sun Y, Heidt T, Vinegoni C, Borodovsky A, Fitzgerald K, Wojtkiewicz GR, Iwamoto Y, Tricot B, Khan OF, Kauffman k. J., Xing Y, Shaw TE, Libby P, Langer R, Weissleder R, Swirski FK, Anderson DG, Nahrendorf M, RNAi targeting multiple cell adhesion molecules reduces immune cell recruitment and vascular inflammation after myocardial infarction. Sci. Transl. Med 8, 342ra380 (2016).

46. Fan Q, Tao R, Zhang H, Xie H, Lu L, Wang T, Su M, Hu J, Zhang Q, Chen Q, Iwakura Y, Shen W, Zhang R, Yan X, Dectin-1 contributes to myocardial ischemia-reperfusion injury by regulating macrophage polarization and neutrophil infiltration. Circulation 139, 663–678 (2018).

47. Wei W, Wang D, Shi J, Xiang Y, Zhang Y, Liu S, Liu Y, Zheng D, Tumor necrosis factor (TNF)-related apoptosis-inducing ligand (TRAIL) induces chemotactic migration of monocytes

via a death receptor 4-mediated RhoGTPase pathway. Mol. Immunol 47, 2475–2484 (2010). [PubMed: 20638129]

48. Van Tassell BW, Canada J, Carbone S, Trankle C, Buckley L, Oddi Erdle C, Abouzaki NA, Dixon D, Kadariya D, Christopher S, Schatz A, Regan J, Viscusi M, Del Buono M, Melchior R, Mankad P, Lu J, Sculthorpe R, Biondi-Zoccai G, Lesnefsky E, Arena R, Abbate A, Interleukin-1 blockade in recently decompensated systolic heart failure: Results from REDHART (Recently Decompensated Heart Failure Anakinra Response Trial). Circ. Heart Fail 10, e004373 (2017).
49. Anker SD, Coats AJ, How to RECOVER from RENAISSANCE? The significance of the results of RECOVER, RENAISSANCE, RENEWAL and ATTACH. Int. J. Cardiol 86, 123–130 (2002). [PubMed: 12419548]
50. Secchiero P, Gonelli A, Corallini F, Ceconi C, Ferrari R, Zauli G, Metalloproteinase 2 cleaves in vitro recombinant TRAIL: Potential implications for the decreased serum levels of TRAIL after acute myocardial infarction. Atherosclerosis 211, 333–336 (2010). [PubMed: 20233617]
51. Aversano T, Zhou W, Nedelman M, Nakada M, Weisman H, A chimeric IgG4 monoclonal antibody directed against CD18 reduces infarct size in a primate model of myocardial ischemia and reperfusion. J. Am. Coll. Cardiol 25, 781–788 (1995). [PubMed: 7860929]
52. Li D, Qiu Z, Shao Y, Chen Y, Guan Y, Liu M, Li Y, Gao N, Wang L, Lu X, Zhao Y, Liu M, Heritable gene targeting in the mouse and rat using a CRISPR-Cas system. Nat. Biotechnol 31, 681–683 (2013). [PubMed: 23929336]
53. Fan L, Kadura I, Krebs LE, Hatfield CC, Shaw MM, Frye CC, Improving the efficiency of CHO cell line generation using glutamine synthetase gene knockout cells. Biotechnol. Bioeng 109, 1007–1015 (2012). [PubMed: 22068567]
54. Cui X, Xie PP, Jia PP, Lou Q, Dun G, Li S, Liu G, Zhang J, Dong Z, Ma Y, Hu Y, Hsf4 counteracts Hsf1 transcription activities and increases lens epithelial cell survival in vitro. Biochim. Biophys. Acta 1853, 746–755 (2015). [PubMed: 25601714]
55. Louch WE, Sheehan KA, Wolska BM, Methods in cardiomyocyte isolation, culture, and gene transfer. J. Mol. Cell. Cardiol 51, 288–298 (2011). [PubMed: 21723873]
56. Yan Y, Jiang W, Liu L, Wang X, Ding C, Tian Z, Zhou R, Dopamine controls systemic inflammation through inhibition of NLRP3 inflammasome. Cell 160, 62–73 (2015). [PubMed: 25594175]
57. Zhao R-R, Ackers-Johnson M, Stenzig J, Chen C, Ding T, Zhou Y, Wang P, Ng SL, Li PY, Teo G, Rudd PM, Fawcett JW, Foo RSY, Targeting chondroitin sulfate glycosaminoglycans to treat cardiac fibrosis in pathological remodeling. Circulation 138, 2497–2513 (2018).
58. Yang P, Han P, Hou J, Zhang L, Song H, Xie Y, Chen Y, Xie H, Gao F, Kang YJ, Electrocardiographic characterization of rhesus monkey model of ischemic myocardial infarction induced by left anterior descending artery ligation. Cardiovasc. Toxicol 11, 365–372 (2011). [PubMed: 21792668]
59. Fink K, Ng C, Nkenfou C, Vasudevan SG, van Rooijen N, Schul W, Depletion of macrophages in mice results in higher dengue virus titers and highlights the role of macrophages for virus control. Eur. J. Immunol 39, 2809–2821 (2009). [PubMed: 19637226]
60. Friedrich V, Flores R, Muller A, Bi W, Peerschke EIB, Sehba FA, Reduction of neutrophil activity decreases early microvascular injury after subarachnoid haemorrhage. J. Neuroinflammation 8, 103 (2011). [PubMed: 21854561]

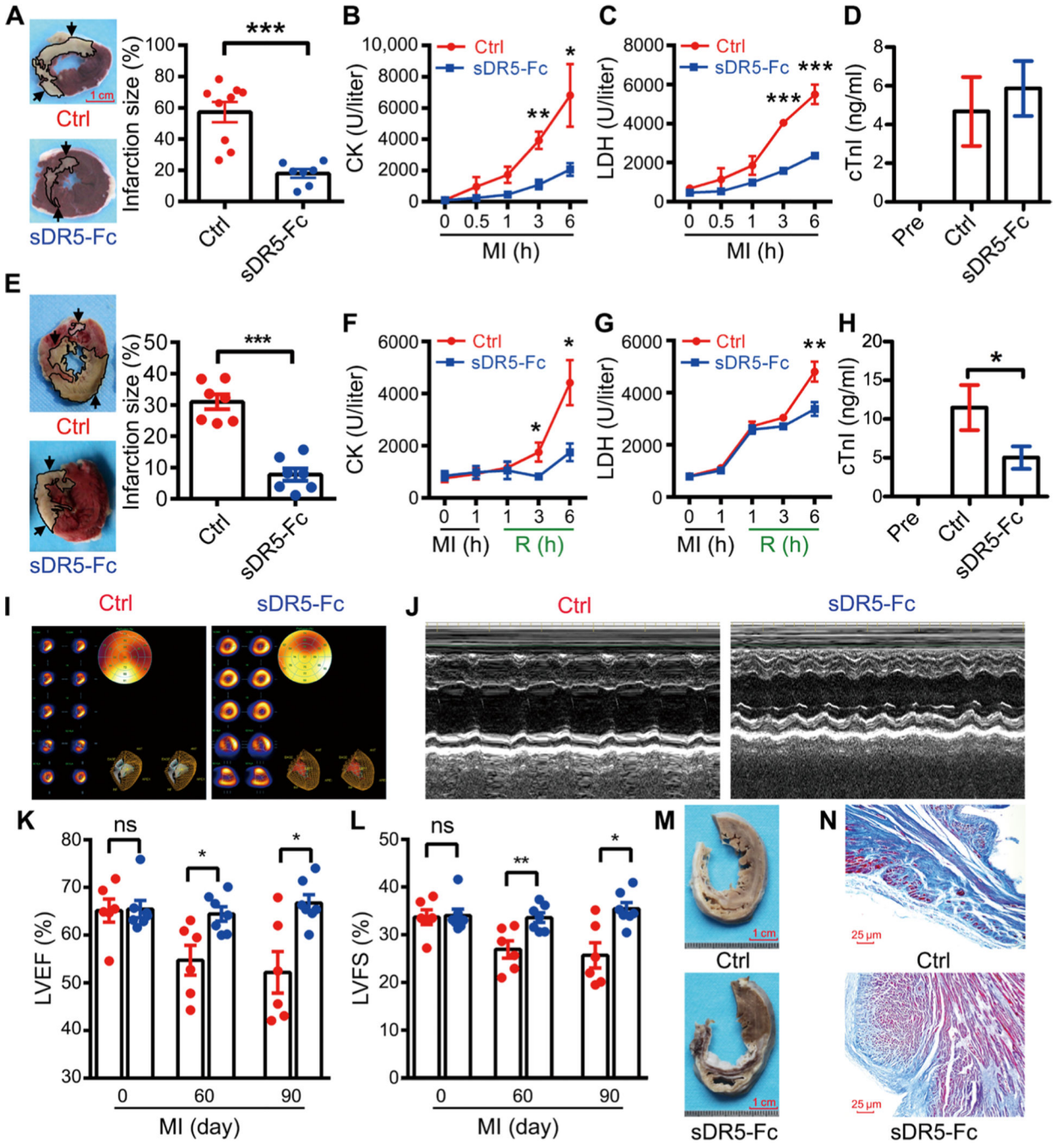

Fig. 1. sDR5-Fc ameliorates myocardial injury and improves ventricular remodeling in monkeys after AMI and I/R.

(**A**) Tetraphenyl tetrazolium chloride (TTC)–stained heart sections 6 hours after LAD ligation in rhesus macaques treated with either control PBS (Ctrl; $n = 9$ monkeys) or sDR5-Fc in PBS ($n = 7$ monkeys) 30 min after LAD ligation. Dead tissue is shown in white (outlined, arrows), whereas viable tissue is shown in red. Quantification of the infarct sizes as percentages of the left ventricles is shown in the right panel; each data point represents one monkey. Scale bar, 1 cm. (**B** to **D**) Plasma concentrations of CK (B), LDH (C), and cTnI

(D) of monkeys treated with PBS (control, $n = 9$ monkeys) or sDR5-Fc ($n = 11$ monkeys), assessed at the indicated times (B and C; analyzed by Catalyst Dx Chemistry Analyzer) or 6 hours after LAD ligation (D; analyzed by ELISA). Pre, pre-LAD ligation plasma. (**E**) TTC-stained heart sections after 1 hour ischemia and 6 hours reperfusion (I1/R6h) in rhesus macaques treated with either PBS (control, $n = 7$ monkeys) or sDR5-Fc in PBS ($n = 7$ monkeys) 5 min before reperfusion. Quantification of the infarct sizes as percentages of the left ventricles is shown in the right panel. Scale bar, 1 cm. (**F** to **H**) Plasma concentrations of CK (F), LDH (G), and cTnI (H) of monkeys treated with PBS (control, $n = 13$ monkeys) or sDR5-Fc ($n = 12$ monkeys), assessed at the indicated times (F and G; analyzed by Catalyst Dx Chemistry Analyzer) or 6 hours after reperfusion (H; analyzed by ELISA). R, reperfusion. (**I**) Representative single-photon emission tomography/computed tomography cardiac images of PBS- or sDR5-Fc–treated monkey hearts 6 hours after LAD ligation. (**J**) Representative echocardiographic M-mode of PBS- or sDR5-Fc–treated monkeys 90 days after LAD ligation. (**K** and **L**) The left ventricle ejection fraction (LVEF) (K) and left ventricle fractional shortening (LVFS) (L) values of PBS- (red circles; $n = 6$ monkeys) or sDR5-Fc–treated monkeys (blue circles; $n = 7$ monkeys) at the indicated times, as measured by echocardiography. ns, not significant. (**M** and **N**) Representative images of heart sections (M; scale bar, 1 cm) and their Masson-stained micrographs (N; scale bar, 25 μm) of PBS- or sDR5-Fc–treated monkeys 90 days after LAD ligation. Quantitative data are shown as means ± SEM. $*P \leq 0.05$, $**P \leq 0.01$, and $***P \leq 0.001$ as determined by two-tailed *t* test (A to C, E to G, and K and L) or one-way ANOVA followed by Tukey's post hoc test (D and H). Results in each group are pooled from all the monkeys used in the group.

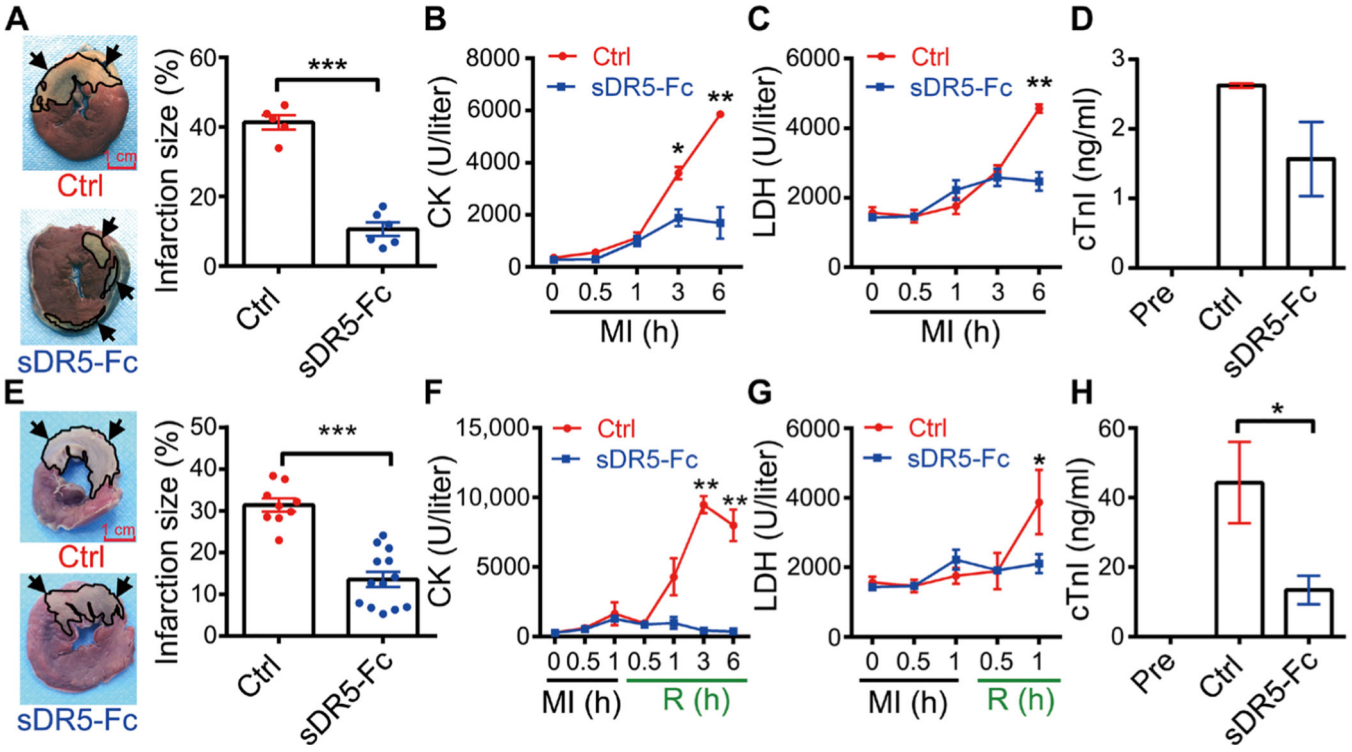

Fig. 2. sDR5-Fc prevents myocardial injury in pigs during AMI and I/R.

(**A**) TTC-stained heart sections 6 hours after LAD ligation in pigs treated with either PBS (Ctrl; $n = 5$ pigs) or sDR5-Fc ($n = 6$ pigs) administered 30 min after LAD ligation. Dead tissue is shown in white (outlined, arrows), whereas viable tissue is shown in red. Quantification of infarct sizes as percentages of the left ventricles is shown in the right panel. (**B** to **D**) Plasma concentrations of CK (B), LDH (C), and cTnI (D) at the indicated times (B and C; analyzed by Catalyst Dx Chemistry Analyzer) or 6 hours (D; analyzed by ELISA) after LAD ligation in pigs treated as described in (A). (**E**) TTC-stained heart sections after I1/R6h in pigs treated with either control PBS ($n = 9$ pigs, top lef) or sDR5-Fc in PBS ($n = 13$ pigs, bottom left) administered 5 min before reperfusion. Quantification of infarct sizes as percentages of the left ventricle is shown in the right panel. (**F** and **H**) Plasma concentrations of CK (F), LDH (G), and cTnI (H) at the indicated times (F and G; analyzed by Catalyst Dx Chemistry Analyzer) or 6 hours (H; analyzed by ELISA) after reperfusion in pigs treated as described in (E). Quantitative data are shown as means ± SEM. $*P \leq 0.05$, $**P \leq 0.01$, and $***P \leq 0.001$ as determined by two-tailed t test (A to C and E to G) or one-way ANOVA followed by Tukey's post hoc test (D and H). Results in each group are pooled from all the pigs used in the group. Scale bar, 1 cm.

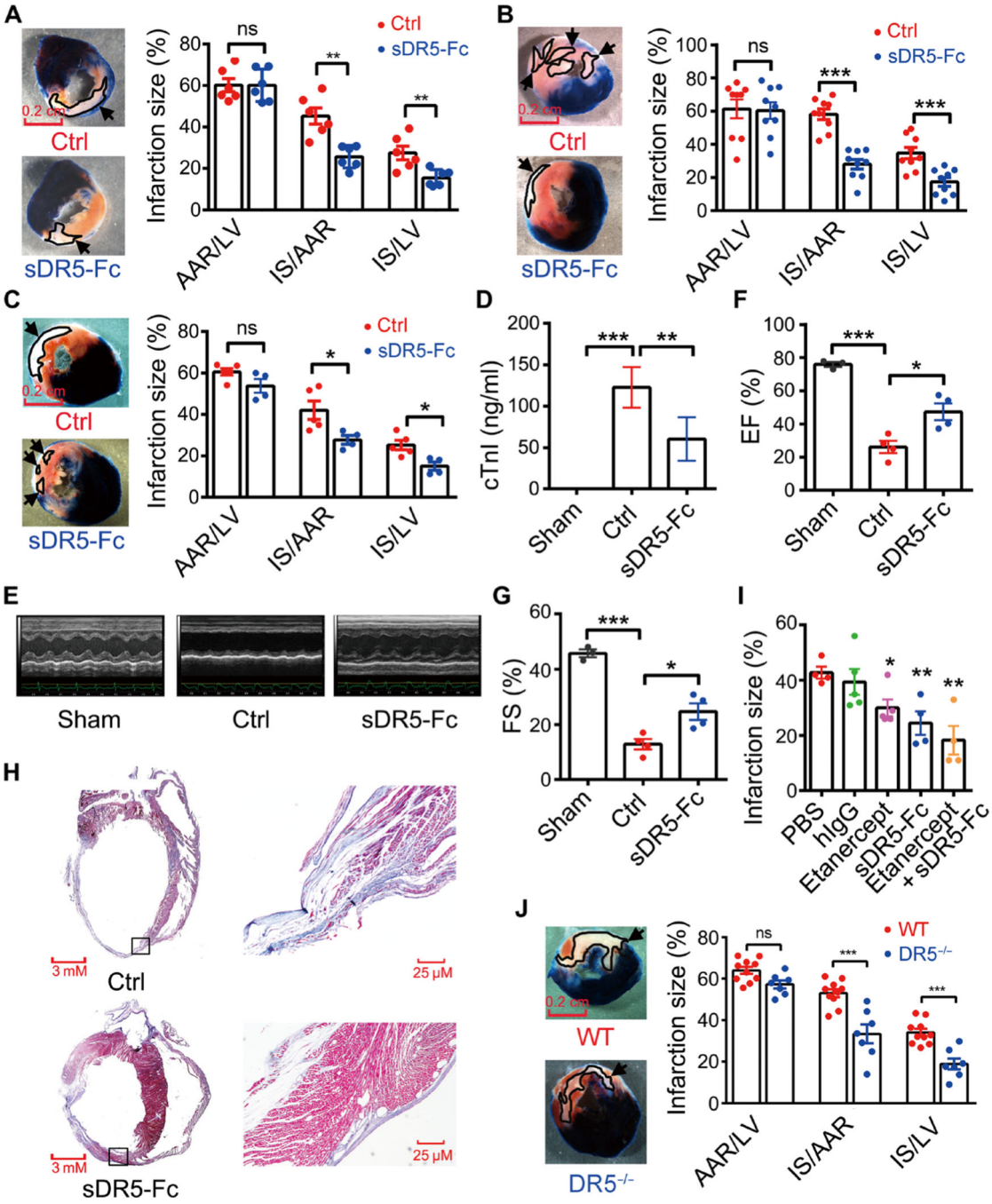

Fig. 3. TRAIL blockade or DR5 gene deletion in rats prevents myocardial injury during AMI and I/R.

(**A**) TTC-Evans blue-stained heart sections 6 hours after LAD ligation in rats treated with either PBS (Ctrl; $n = 6$ rats) or sDR5-Fc in PBS ($n = 6$ rats) administered 30 min after LAD ligation. Quantification of infarct sizes as percentages of the left ventricle is show in the right panel. AAR, area at risk (blue); IS, infarction size (white); LV, left ventricle (blue, white, and red). (**B**) TTC-Evans blue-stained heart sections after I1/R3h in rats treated with either PBS ($n = 9$ rats) or sDR5-Fc in PBS ($n = 9$ rats) administered 5 min before

reperfusion. Quantification of infarct sizes as percentages of the left ventricle is shown in the right panel. (**C**) TTC-Evans blue-stained heart sections after I1/R24h in rats treated with either control PBS ($n = 5$ rats) or sDR5-Fc in PBS ($n = 4$ rats) administered 5 min before reperfusion. Quantification of infarct sizes as percentages of the left ventricle is shown in the right panel. (**D**) Serum cTnI concentrations in sham- ($n = 5$ rats), PBS- ($n = 4$ rats), and sDR5-Fc–treated rats ($n = 6$ rats) after I1/R3h, as determined by ELISA. (**E**) Representative echocardiography images of sham-, PBS-, and sDR5-Fc–treated rats 4 weeks after LAD ligation. (**F** and **G**) The EF and FS values measured by echocardiography 4 weeks after LAD ligation in sham- ($n = 3$ rats), control PBS- ($n = 4$ rats), and sDR5-Fc–treated rats ($n = 4$ rats). (**H**) Masson's trichrome–stained heart sections 4 weeks after LAD ligation in PBS- and sDR5-Fc–treated rats. Boxed regions are shown at higher magnification on right. (**I**) Infarct sizes of rats after I1/R24h treated with PBS ($n = 4$ rats), human IgG ($n = 5$ rats), etanercept ($n = 5$ rats), sDR5-Fc ($n = 4$ rats), or etanercept + sDR5-Fc ($n = 4$ rats), administered 5 min before reperfusion. (**J**) TTC-Evans blue-stained heart sections after I1/R24h in wild-type (WT; $n = 10$ rats) or $DR5^{-/-}$ rats ($n = 7$ rats). Quantification of infarct sizes as percentages of the left ventricle is shown in the right panel. Quantitative data are shown as means ± SEM. $^{*}P \leq 0.05$, $^{**}P \leq 0.01$, and $^{***}P \leq 0.001$ as determined by two-tailed *t* test (A to C and J) or one-way ANOVA followed by Tukey's post hoc test (D, F, G, and I). The experiments were repeated at least three times with similar results. Scale bars, 0.2 cm.

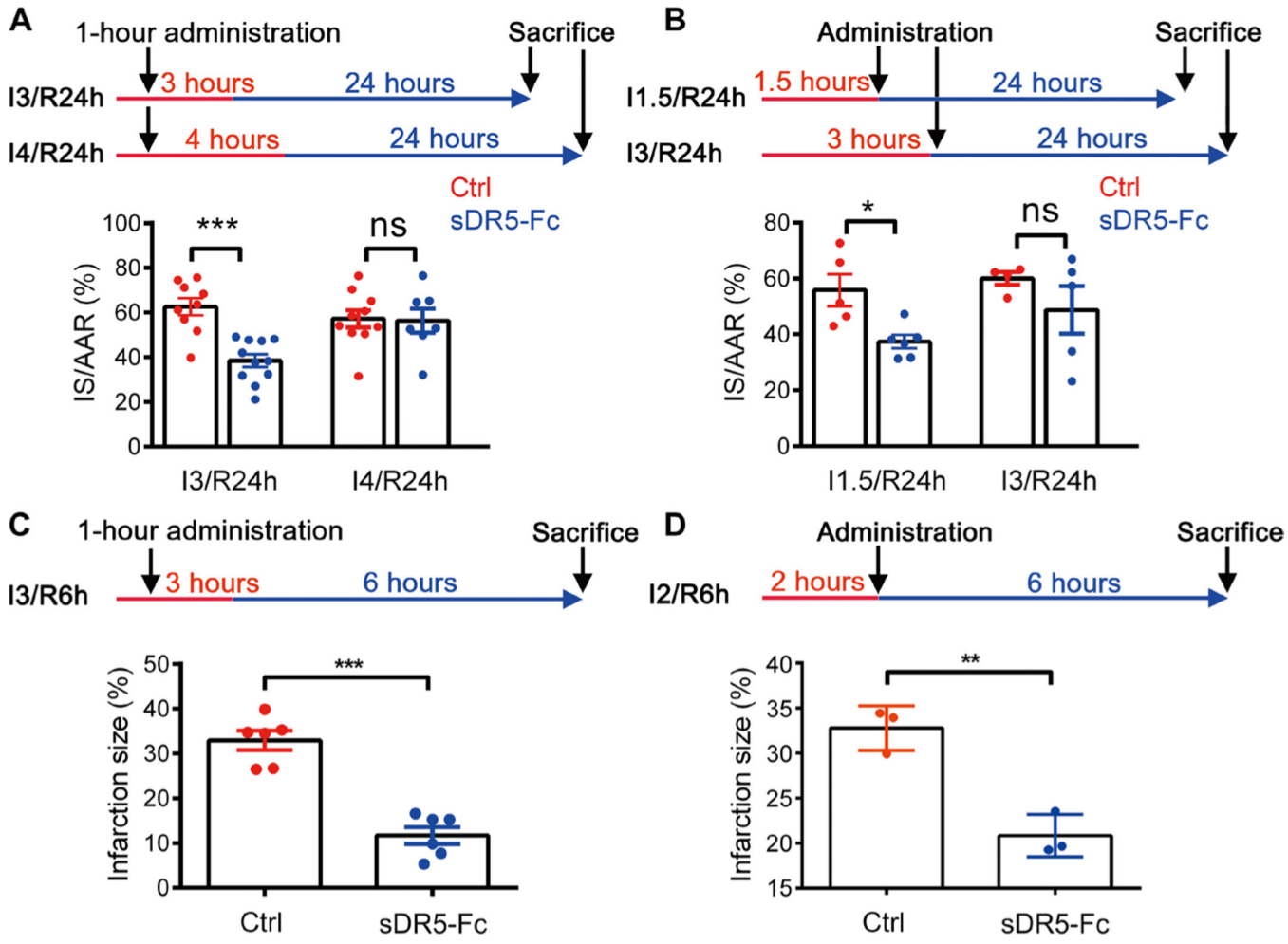

Fig. 4. Timing of therapeutic intervention with sDR5-Fc for cardiac ischemia in rats and monkeys.

(**A**) Schematic of sDR5-Fc administration 1 hour after ligation in the Wistar rat model. Bottom panel shows quantification of infarct sizes as percentages of IS/AAR in TTC-Evans blue-stained heart sections after I3/R24h and I4/R24h in rats treated with either PBS (n = 9 in I3/R24h model and n = 10 in I4/R24h model) or sDR5-Fc in PBS (n = 11 in I3/R24h model and n = 7 in I4/R24h model) administered 1 hour after ligation. (**B**) Schematic of sDR5-Fc administration 1.5 or 3 hours after ligation in the Wistar rat model. Bottom panel shows quantification of infarct sizes as percentages of IS/AAR of TTC-Evans blue-stained heart sections after I1.5/R24h and I3/R24h in rats treated with either PBS (n = 5 in I1.5/R24h model and n = 4 in I3/R24h model) or sDR5-Fc in PBS (n = 6 in I1.5/R24h model and n = 5 in I3/R24h model) administered 5 min before reperfusion. (**C**) Schematic of sDR5-Fc administration 1 hour after ligation in rhesus macaques. Bottom panel shows quantification of infarct sizes as percentages of the left ventricle of TTC-stained heart sections after 3-hour ischemia and 6-hour reperfusion (I3/R6h) in rhesus macaques treated with either PBS (n = 6 monkeys) or sDR5-Fc in PBS (n = 6 monkeys) administered 1 hour after ligation. (**D**) Schematic of sDR5-Fc administration 2 hours after ligation in rhesus macaques. Bottom panel shows quantification of infarct sizes as percentages of the left ventricle of TTC-stained

heart sections after 2-hour ischemia and 6-hour reperfusion (I2/R6h) in rhesus macaques treated with either PBS (n = 3 monkeys) or sDR5-Fc in PBS (n = 3 monkeys) administered 5 min before reperfusion. Each data point represents one animal. Red line represents ischemic time, and blue line represents reperfusion time. Quantitative data are shown as means ± SEM. *$P \leq 0.05$, **$P \leq 0.01$, and ***$P \leq 0.001$ as determined by two-tailed t test. Data for rats are representative of three independent experiments (A and B), and data for monkeys are pooled from all animals used (C and D).

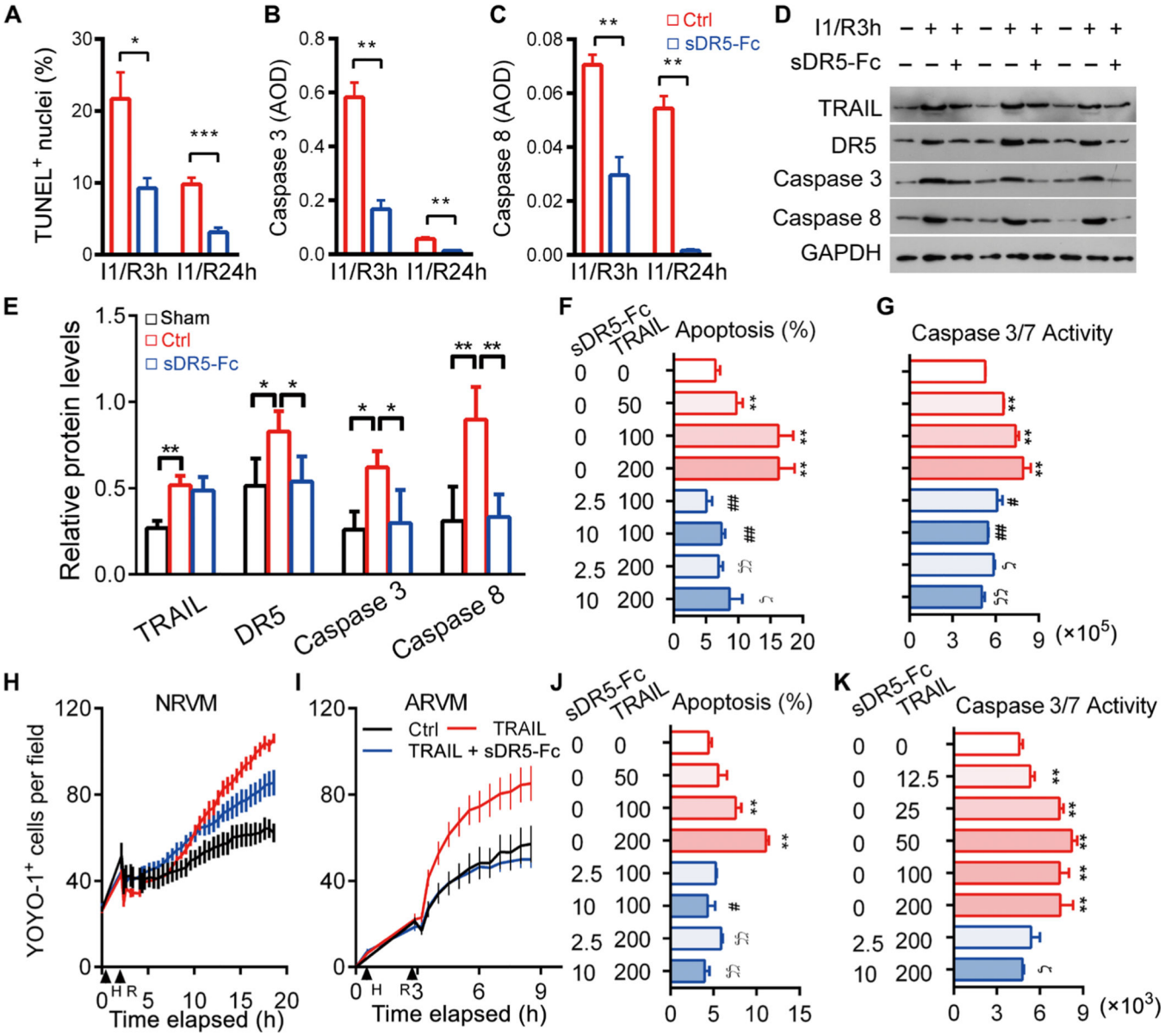

Fig. 5. sDR5-Fc protects rat and human cardiomyocytes from TRAIL-induced death.

(**A**) Percent TUNEL$^+$ nuclei in rat heart sections after I1/R3h or I1/R24h with or without sDR5-Fc treatment ($n \geq 3$ mice). (**B** and **C**) Caspase 3 (B) and caspase 8 (C) expressions as determined by IHC of heart sections described in (A) ($n \geq 3$ per group). AOD, average optical density. (**D** and **E**) Immunoblot micrographs (D) and quantification (E) of rat heart homogenates after I1/R3h or I1/R24h with or without sDR5-Fc treatment, for DR5, TRAIL, activated caspase 3, activated caspase 8, and glyceraldehyde-3-phosphate dehydrogenase (GAPDH). Each lane represents one rat ($n \geq 3$ rats). (**F**) Percent apoptotic cells as determined by TUNEL staining in NRVM cultures treated with TRAIL or sDR5-Fc as indicated under the H2/R3h stress condition. $n \geq 5$ cultures. (**G**) Caspase 3/7 activity as determined by Caspase-Glo3/7 assay presented as relative luminescence unit (RLU) in cultures described in (F). (**H** and **I**) Number of dead cells per field of NRVMs and

ARVMs treated with or without TRAIL or sDR5-Fc as determined by YOYO-1 dye staining and time-lapse microscopy with 30-min intervals. (**J** and **K**) Percent apoptotic cells as determined by TUNEL (J) and caspase 3/7 activity by Caspase-Glo3/7 assay (K) in human cardiac myocyte cultures treated with TRAIL or sDR5-Fc as indicated under the H3/R3h stress condition ($n \geq 3$ cultures). Data are shown as means ± SEM. Statistical significance was determined by two-tailed *t* test (A to C) or one-way ANOVA followed by Tukey's post hoc test (E to G and J to K). *$P < 0.05$, **$P < 0.01$, #$P < 0.05$, and ##$P < 0.01$ versus TRAIL group (100 ng/ml); Ϛ$P < 0.05$ and ϚϚ$P < 0.01$ versus TRAIL group (200 ng/ml).

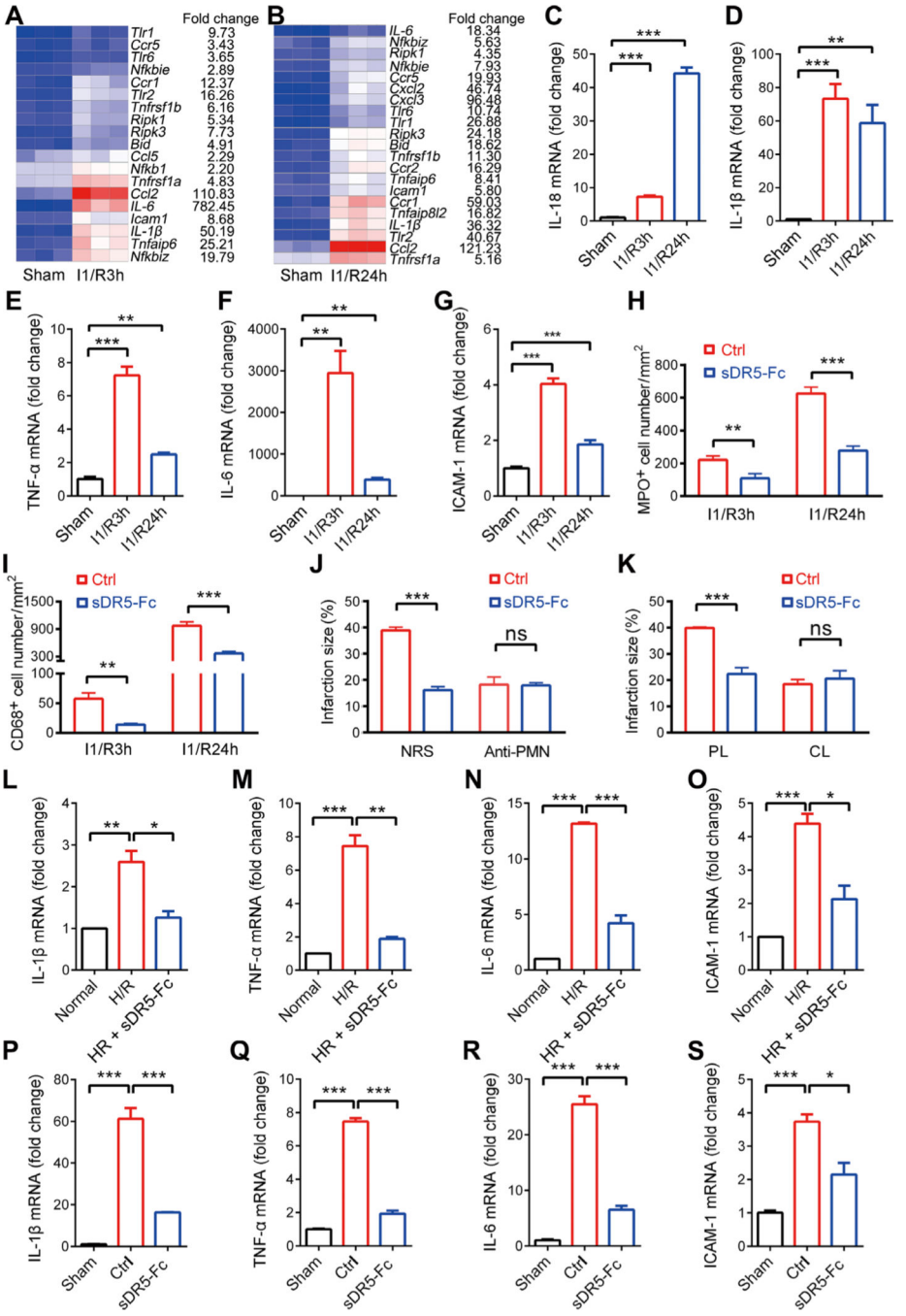

Fig. 6. The effect of sDR5-Fc on cardiac I/R is dependent on myeloid cells.

(**A** and **B**) Heat map of RNA-seq data of rat heart tissue from sham or ischemic animals. Each column represents three rats. (**C** to **G**) mRNA expression of *IL-18*, *IL-1*β, *TNF*-α, *IL-6*, and *ICAM-1* in the myocardium of sham or ischemic rats as detected by quantitative PCR. (**H** and **I**) Numbers of MPO^+ (H) and $CD68^+$ (I) cells per mm^2 of rat heart sections after the indicated treatments as determined by IHC ($n \geq 3$ rats). (**J**) Infarct size as a percentage of the left ventricle in rats pretreated with a neutrophil-depleting antibody or normal rabbit serum (NRS) followed by I1/R24h with or without sDR5-Fc injection (5 min

before reperfusion; $n \geq 4$ rats). (**K**) Infarct size as a percentage of the left ventricle in rats pretreated with macrophage- depleting clodronate liposomes (CL) or control liposomes (PL) followed by I1/R24h with or without sDR5-Fc injection (5 min before reperfusion; $n \geq 4$ rats). (**L** to **O**) mRNA expression of proinflammatory molecules in rat macrophage cell line NR8383 after hypoxia for 1 hour followed by reoxygenation for 3 hours, with or without sDR5-Fc during both hypoxia and reoxygenation, as determined by real-time PCR ($n = 3$) cultures. (**P** to **S**) mRNA expression of proinflammatory molecules in isolated cardiac infiltrating myeloid cells of rats after I1/R24h with or without sDR5-Fc administration (5 min before reperfusion), as determined by real-time PCR ($n = 3$ mice). Data are shown as means ± SEM. $^{*}P \leq 0.05$, $^{**}P \leq 0.01$, and $^{***}P \leq 0.001$ as determined by two-tailed t test (I to K) or one-way ANOVA followed by Tukey's post hoc test (C to H and L to S). The experiments were repeated at least three times with similar results.

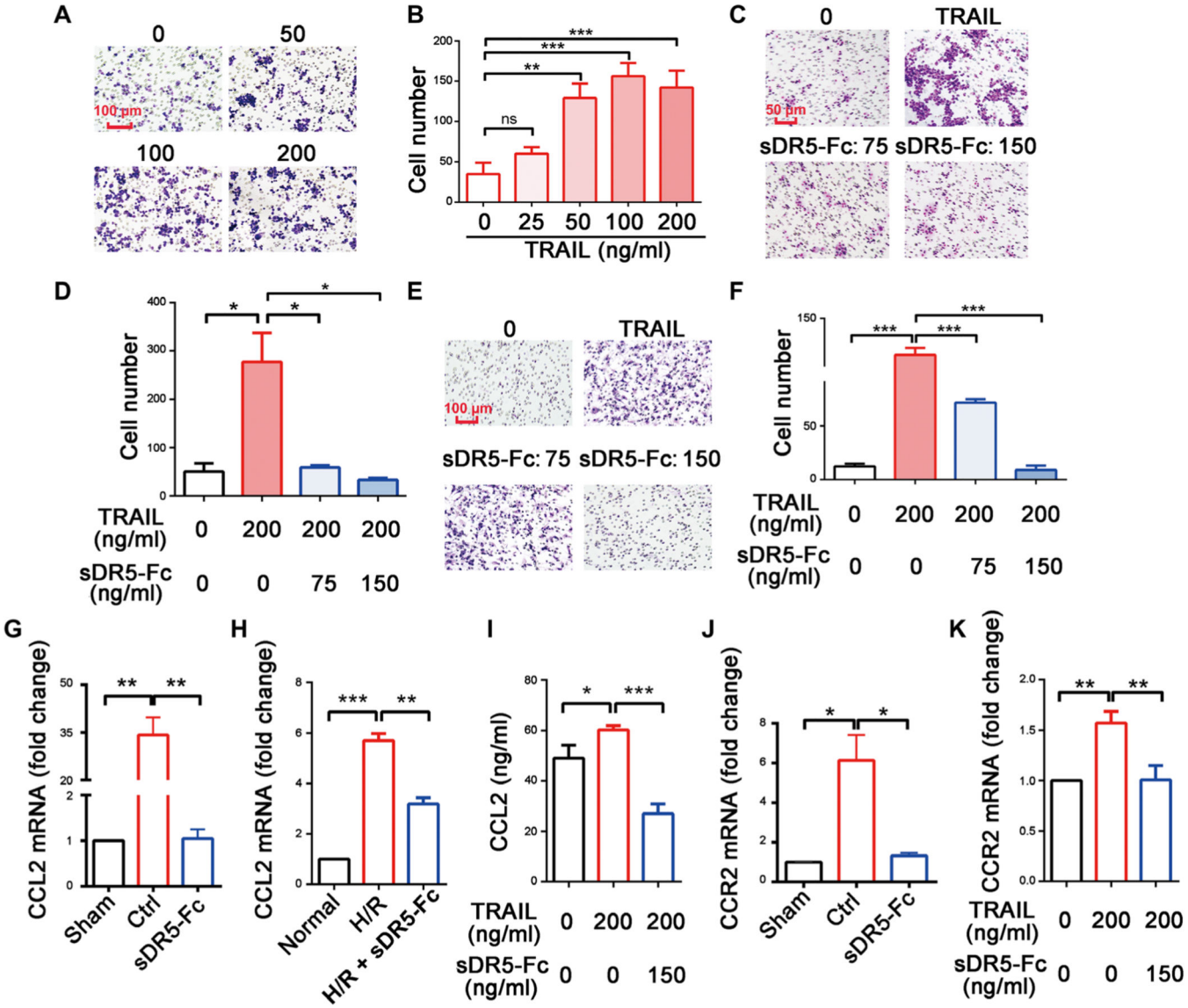

Fig. 7. TRAIL is a chemoattractant for myeloid cells.

(**A** and **B**) Representative images of migrating NR8383 cells in response to the indicated concentrations of TRAIL in a Transwell assay (A) and the quantification of the results (B). Scale bar, 100 μm. (**C** and **D**) Representative images of migrating NR8383 cells in the presence of the indicated concentrations of TRAIL or sDR5-Fc in a Transwell assay (C) and the quantification of the results (D). Scale bar, 50 μm. (**E** and **F**) Representative images of migrating rat BMDMs in the presence of the indicated concentrations of TRAIL or sDR5-Fc in a Transwell assay (E) and the quantification of the results (F). Scale bar, 100 μm. (**G** and **H**) The expression of *CCL2* mRNA in the left ventricles of rat hearts after I1/R24h (G; sDR5-Fc was administered 5 min before reperfusion) and in NR8383 cells treated with hypoxia/reoxygenation (H/R) and/or sDR5-Fc (H; sDR5-Fc was present during both hypoxia and reoxygenation). (**I**) The concentrations of CCL2 protein in the supernatant of BMDMs treated with TRAIL and/or sDR5-Fc as determined by ELISA. (**J** and **K**) The expressions of *CCR2* mRNA in the left ventricles of rat hearts after I1/R24h (J; sDR5-Fc

was administered 5 min before reperfusion) and in NR8383 cells (K; sDR5-Fc was present during both hypoxia and reoxygenation) treated with TRAIL and/or sDR5-Fc. Data are shown as means ± SEM.*$P \leq 0.05$, **$P \leq 0.01$, and ***$P \leq 0.001$ as determined by one-way ANOVA followed by Tukey's post hoc test. The experiments were repeated at least three times with similar results.